

Sensitivity of Modeled Number Concentrations to the Representation of New Particle Formation and Particle Emissions in Chemical Transport Models

Lim-Seok Chang, Douglas L. Wright, Ernie R. Lewis, Stephen E. Schwartz, and Robert McGraw
Atmospheric Science Division, Brookhaven National Laboratory, 11973, USA

INTRODUCTION

Uncertainties in new particle formation (NPF) and emissions rates for particle number yield large uncertainties in modeled number concentrations (N). In this study, sensitivity studies were performed with a variety of approaches to NPF and several number emission rates using the Community Multiscale Air Quality (CMAQ) regional-scale model over all of the continental U.S with 60-km resolution for July 2004..

MODEL DESCRIPTION

NPF approaches included binary $\text{H}_2\text{SO}_4\text{-H}_2\text{O}$ nucleation (Vehkamaki *et al.*, 2002; V02), ternary $\text{H}_2\text{SO}_4\text{-H}_2\text{O-NH}_3$ nucleation (Napari *et al.*, 2002; N02), and nucleation by ion-ion recombination (Turco *et al.*, 1998; NIIR). Newly-formed particles entered the Aitken mode at 3 nm diameter. The Kerminen and Kulmala (2002) parameterization for the ratio F_{KK02} of the NPF rate J_p at d_{npf} (3 nm in this work) to the nucleation rate J (1 nm) was included in some model variants. Empirical rates for the formation of 3–4 nm particles under clean conditions of the form $J_p = K[\text{H}_2\text{SO}_4]^n$, $n=1, 2$ (Eisele and McMurry, 1997; EM97) were also included. After calculating $J_p = F_{\text{KK02}} J$ or $J_p = J$, the (constant) J_p over the 15-min time step was limited by the available H_2SO_4 .

RESULTS

Overall model sensitivities were examined using average J_p and N over the domain and simulated period ($J_{p, \text{ave}}$ and N_{ave}). The basecase J_p was the sum of the N02 and NIIR rates reduced by the factor F_{KK02} . Key results follow.

1. Using $J_p = F_{\text{KK02}} J$ rather than $J_p = J$ reduced $J_{p, \text{ave}}$ by a factor of ~ 3 and N_{ave} by a factor of ~ 2 , even though the conversion is only to slightly larger (3-nm) size.
2. Replacing the ternary rate with the binary rate decreased $J_{p, \text{ave}}$ by a factor ~ 0.05 but decreased N_{ave} by only ~ 0.4 . Binary nucleation was usually negligible in the boundary layer (PBL); above the PBL the extent of binary nucleation approached that of ternary nucleation because of lower temperatures and $[\text{NH}_3]$.
3. When the binary nucleation rate was used, inclusion of NIIR increased both $J_{p, \text{ave}}$ and N_{ave} only modestly.
4. The NPF rate of the average of the two $n = 2$ curves of Fig. 7 of EM97 yielded $J_{p, \text{ave}}$ intermediate between that of the binary and ternary parameterizations in the PBL, and comparable to the binary $J_{p, \text{ave}}$ above the PBL.

5. Reducing the mean diameter of emitted particles by a factor of two (for fixed mass emission rate) for both the Aitken and accumulation modes gave a modest decrease in both $J_{p, \text{ave}}$ and N_{ave} . This resulted from increased surface area and reduced NPF when emitted mass is apportioned into smaller particles. Increasing the emitted mean diameter increased $J_{p, \text{ave}}$ and N_{ave} .
6. Particle transfer from the Aitken to the accumulation mode is necessary in modal models to maintain distinct modes. Transfer is not governed by a physical process, and for large NPF rates this introduces a substantial uncertainty in accumulation mode number.
7. When the NPF rate is large, the subsequent reduction of J_p due to limited H_2SO_4 was also large with the 15-min time step. Nucleation and condensation are partially operator-split in CMAQ. When its binary nucleation rate is replaced by the N02 ternary rate, H_2SO_4 consumption is biased in favor of NPF.
8. In the Aitken mode, average NPF and coagulation rates nearly balanced. In the accumulation mode, number emissions and intermodal transfer were balanced by wet deposition.

CONCLUSIONS

New particle formation dominates uncertainties in Aitken mode number concentration, whereas conversion of mass emission rates to number emission rates dominates uncertainties in accumulation mode number.

Keywords: *New particle formation*

REFERENCES

- Eisele, F. L., McMurry, P. H. (1997). Recent progress in understanding particle nucleation and growth, *Phil. Trans. R. Soc. Lond.* B 252, 191-201.
- Napari, I., Noppel, M., Vehkamaki, H., Kulmala, M. (2002). Parameterization of ternary nucleation rates for $\text{H}_2\text{SO}_4\text{-NH}_3\text{-H}_2\text{O}$ vapors, *J. Geophys. Res.*, 107, D19, 4831, doi:10.1029/2002JD002132.
- Turco, R. P., Zhao, J. X., Yu, F. (1998). A new source of tropospheric aerosols: Ion-ion recombination, *Geophys. Res. Letters*, 25, 635-638.
- Vehkamaki, H., Kulmala, M., Napari, I., Lehtinen, K. E. J., Timmreck, C. Noppel, M., and Laaksonen, A. (2002). An improved parameterization for sulfuric acidwater nucleation rates for tropospheric and stratospheric conditions, *J. Geophys. Res.*, 107, D22, 4622, doi:10.1029/2002JD002184.

INTRODUCTION : The sensitivity of modeled number concentrations to particle sources was examined with the Community Multiscale Air Quality (CMAQ) modeling system for the continental U.S. at 60-km resolution and for the northeast U.S. at 12-km resolution. The two sources of particle number, primary particle emissions and secondary particle formation from gaseous precursors, are both subject to large uncertainties. The derivation of number emission rates from inventory mass emission rates requires assumption of an average emitted particle size. Theoretical nucleation rates necessary to calculate ultrafine particle formation rates vary widely among mechanisms and parameterizations. With modal aerosol size representations (as in CMAQ), calculation of CCN number concentration is typically based upon accumulation mode number concentration and sensitive to these uncertainties.

1. Model Variants and Budget Analysis

Model Variant		Parameterizations Included	
M1	N02	NIIR	F_{KK02}
M2	N02	NIIR	F_{KK02}
M3	N02	NIIR	F_{KK02}
M4	N02	NIIR	F_{KK02}
M5	V02	NIIR	F_{KK02}
M6	V02	NIIR	F_{KK02}
M7	V02	NIIR	F_{KK02}
M8	JVM	NIIR	F_{KK02}
M9	N02	NIIR	F_{KK02}
M10	N02	NIIR	F_{KK02}
M11	N02	NIIR	F_{KK02}
M12	EM97	NIIR	F_{KK02}

Parameterizations		
JVM	Binary $H_2SO_4-H_2O$ nucleation rate: J Jaeger-Voroi and Mirabel, 1989	theory
V02	Binary $H_2SO_4-H_2O$ nucleation rate: J Vehkamäki et al., 2002	theory
N02	Ternary $H_2SO_4-H_2O-NH_3$ nucleation rate: J Napari et al., 2002	theory
NIIR	Ion-ion recombination nucleation rate: J Turco et al., 1998	theory
F_{KK02}	New particle formation rate: $J_p = F_{KK02} J$ Kerminen and Kulmala, 2002	theory
EM97	New particle formation rate: $J_p = K[H_2SO_4]^2$ Eisele and McMurry, 1997	empirical

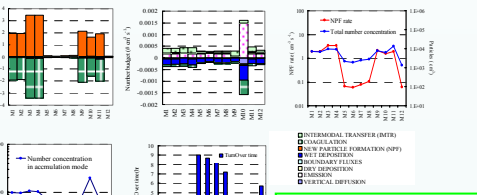


Fig.1 Domain- and time-averaged number budgets, new particle formation rate, number concentrations, and Aitken mode turnover time for each model variant.

COMMENTS
 1. The range of variation in average total number concentration over the model variants is an order of magnitude smaller than the range of variation in average particle formation rates.
 2. The uncertainty in average number concentration in the accumulation mode is due largely to uncertainty in the conversion of mass emission rates to number emissions rates rather than to uncertainty in new particle formation rates

2. Geographical Distributions

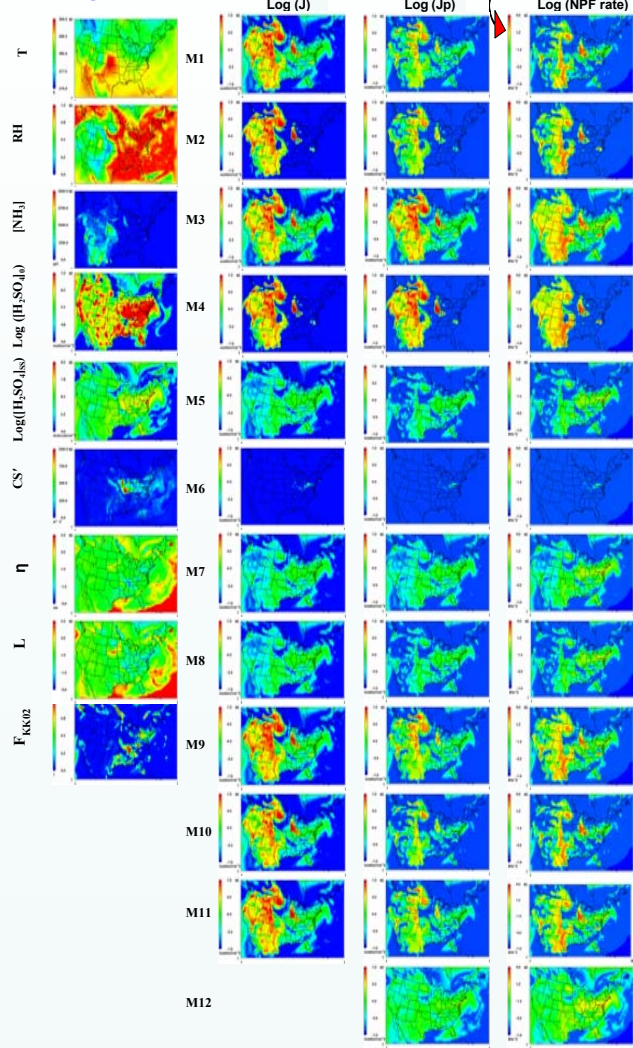


Fig.2 Snapshot of T, RH, $[NH_3]$, $[H_2SO_4]$, CS' , η , L , F_{KK02} (first column), J (second column), J_p (third column) and NPF rate (fourth column) for each model variant at 15UTC on July 6, 2004 at 600 m altitude. Values are from the base case simulation.

$[H_2SO_4]_0$ sulfuric acid concentration after 15 min of chemistry and before aerosol microphysics
 $[H_2SO_4]_{ss}$ steady state sulfuric acid concentration used to calculate J
 CS' condensational sink
 H ratio of condensation sink to growth rate
 J nucleation rate
 J_p particle formation rate before $[H_2SO_4]$ mass limitation
 NPF particle formation rate limited by available $[H_2SO_4]$
 L dimensionless criterion for new particle formation (McMurry et al., JGR, 2005)

COMMENTS
 1. NIIR is important if both $[H_2SO_4]$ and $[NH_3]$ are relatively low.
 2. Time step size, partial operator splitting between NPF and condensational growth, and rapidly changing conditions result in initial overestimation of the NPF rate. Subsequent limitation of the NPF rate by H_2SO_4 availability reduces initial rates by as much as a factor of 1000.
 3. Empirical curves taken from EM97 yield widespread NPF over much of the continent. NPF rates are typically between those derived from binary and ternary nucleation parameterizations.

3. NPF rate and L

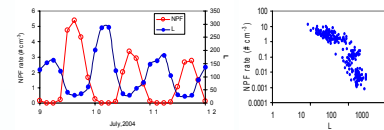


Fig.3 Left: Time series of NPF rate and L over 9-12 July 2004. Right: Scatter plot of NPF rate versus L over all July. NPF rate and L are averaged for all grid boxes and time steps for which $[H_2SO_4]_{ss} \geq 10^4$ molecules cm^{-3} .

COMMENTS
 Both plots illustrate a reciprocal relationship between L and NPF rate.

4. Comparison with Observations



Fig.4 Time series for selected ICARTT flights. First row: altitude. Second: modeled and observed surface area concentrations. Third: modeled and observed volume concentrations. Model results were interpolated in x, y, z, and t for comparison with observations. Results are shown for M1 at 12-km resolution, and M1 and M12 at 60-km resolution. All observations were from NASA DC-8 flights on July 5, 9, 11, 15, 20, 21 and 25, 2004.

COMMENTS
 Modeled number concentrations track the observations more closely than surface area or volume concentrations.